Schottky Quantum Dot Solar Cells Stable in Air under Solar Illumination

By *Jiang Tang, Xihua Wang, Lukasz Brzozowski, D. Aaron R. Barkhouse, Ratan Debnath, Larissa Levina,* and *Edward H. Sargent**

Colloidal quantum dots (CQDs) solar cells[1,2] offer great potential in solar energy conversion in view of their compatibility with solution processing, enabling rapid, large-area, low-cost fabrication. Compared with organic and polymer solar cells also benefiting from solution-processing, solar cells based on PbS,[3–5] PbSe,[6,7] and PbSSe[8] CQDs access a greater portion of the sun's spectrum in the infrared range through the use of low-bandgap PbS and PbSe nanoparticles.

A specific solar cell architecture—a planar film of p-type colloidal quantum dots topped by a shallow-work-function contact, producing a Schottky barrier that generates a depletion region for carrier separation[9]—has seen rapid recent progress. Monochromatic power conversion efficiencies (MPCE) have now reached 4.2% in the infrared[9] and AM1.5G power conversion efficiencies (AM1.5G PCE) have reached 3.3%.[8]

This otherwise promising class of photovoltaics suffers a major limitation: every report details a lack of stability in air, though different reasons have been given. The first high-efficiency reports employed butylamine capped PbS nanoparticles[3] and degraded in air within minutes; the butylamine was suspected of reacting with the shallow-work-function metal contact. Passivating PbSe using 1,4-benzenedithiol led to devices stable in a glovebox over weeks, and in air over a few hours, a considerable improvement.[7] Other reports using ethanedithiol (EDT)[6,10] indicated that even minutes' removal of the devices from a glovebox produced rapid degradation.

Two general areas of possible degradation may be posited:

i) Within the film itself: The film of CQDs may lose passivation and/or develop midgap recombination centers. Labile ligands such as butylamine and ethanedithiol makes the film particularly vulnerable to attack by oxygen and moisture; and the finding of increased lifetime in devices employing the more robust 1,4-benzenedithiol suggests that the stability of passivation within the film may indeed play a key role.

ii) At the film-metal interface: Shallow-work-function metals are known to be oxidized rapidly; they also may react with ligands in the film.

In work on photoconductors, we have found that PbS CQDs, passivated using a wide variety of ligands (amines, thiols, dithiols), but electrically contacted using deep-work-function metals such as Au and ITO,[11–13] suffered no such rapid catastrophic decay in air. These findings pointed to hypothesis 2) above, i.e., a key role for the Schottky barrier. This hypothesis is also consistent with Gur and Alivisatos' remarkably air- and photo-stable heterojunction CQDs device that did not rely on Schottky contacts.[1,2]

We first sought a more definitive understanding of whether the bulk PbS film or the PbS film/Al electrode interface provides the weakest link in device stability. We fabricated PbS nanocrystal solar cells using ITO as anode and either Al or Ag as the Schottky contact. PbS film was produced using a modified layer-by-layer (LBL) deposition technique.[14] All CQD film processing and device testing reported in this work were carried out in a room air ambient without any encapsulation. To ensure persuasive comparison between Al versus Ag contacts, a single film was grown and divided into two pieces and Al was deposited on one piece, Ag on the other. Devices were stored on lab bench without any encapsulation or light shielding and we tracked their performance to compare air stability of devices having different metal cathodes.

The evolution of device performance in time is shown in Figure 1. As seen in Figure 1A, the Al devices degraded rapidly in open-circuit voltage (V_{oc}), external quantum efficiency (EQE) at 632 nm, and fill factor (FF) during ambient storage, leading to a complete loss of MPCE over 4 days. This device actually compares favorably with PbSe-EDT devices for which near-instantaneous degradation has been reported upon exposure to air.[6,10] We proposed two explanations for the improved air stability: i) we work with PbS, known to be less air-sensitive;[15] ii) the devices are fabricated in air and annealed at 90 °C in air for 5 min, resulting in some pre-oxidation of the materials prior to contact deposition.

Strikingly, devices using Ag contacts showed significant improved air-stability: after 4 days' ambient storage, the EQE, V_{oc}, FF and MPCE decreased to 58%, 87%, 83%, and 42% of their initial values, respectively. If we define the lifetime of a cell as the duration of its survival to within 80% of its initial MPCE value, the Al device lifetime was slightly under 4 h. By the same criterion, devices using Ag electrodes had lifetimes of 50 h, a 12-fold improvement in device longevity.

[*] Prof. E. H. Sargent, Dr. X. Wang, Dr. L. Brzozowski, Dr. D. A. R. Barkhouse, Dr. R. Debnath, Dr. L. Levina
Department of Electrical and Computer Engineering
University of Toronto
10 King's College Road, Toronto, Ontario M5S 3G4 (Canada)
E-mail: ted.sargent@utoronto.ca
J. Tang
Department of Materials Science and Engineering
184 College Street, Toronto, Ontario M5S 3E4 (Canada)

DOI: 10.1002/adma.200903240

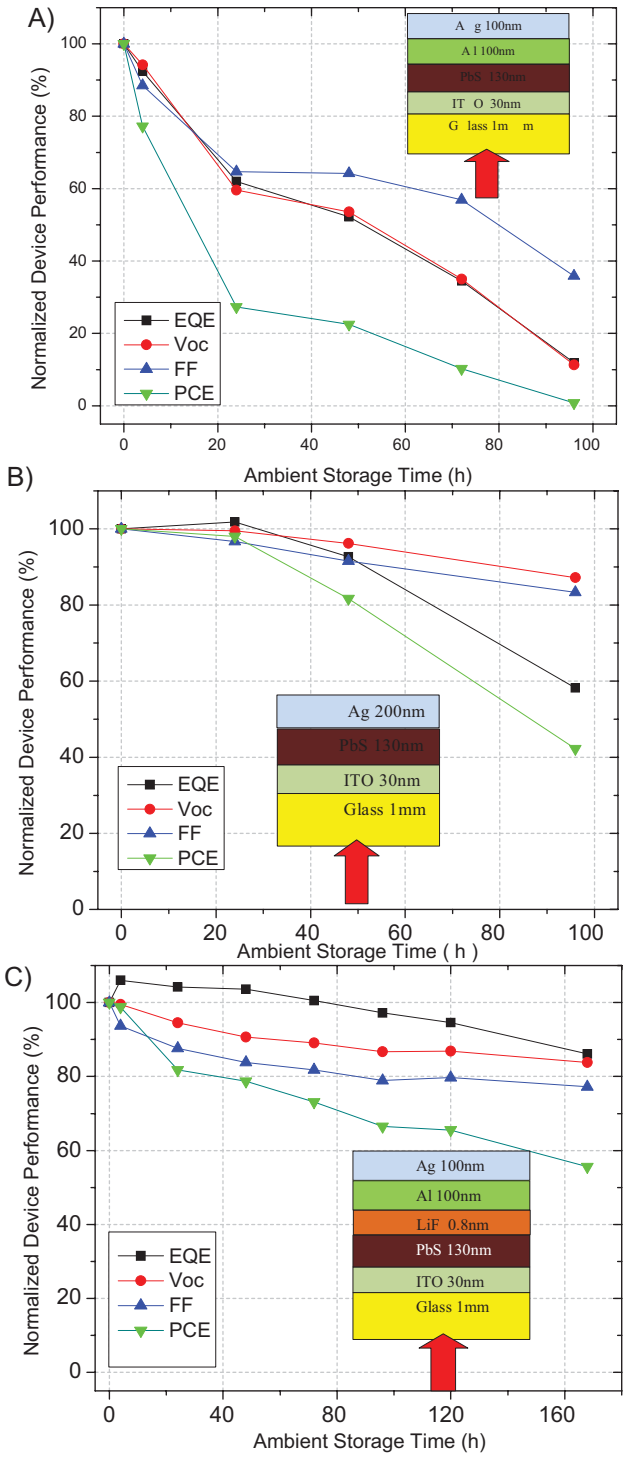

Figure 1. Normalized device performance (EQE, V_{oc}, FF, and MPCE) as a function of ambient storage time for PbS solar cells using different cathodes: A) Al/Ag, B) Ag, and C) 0.8 nm LiF/Al/Ag. Corresponding device architectures are schematically shown as insets. All devices were tested in air under 120 mW cm^{-2} monochromatic 632-nm-wavelength illumination from the ITO side. The initial absolute EQE, V_{oc}, FF and MPCE of Al/Ag, pure Ag and LiF/Al/Ag devices are: 38.1%, 0.42 V, 48% and 4.1%; 24.5%, 0.24 V, 27% and 0.78%; 40.2%, 0.52 V, 54.5% and 5.8%; respectively. Data shown in each panel are representative of 8 devices tested.

Since the Al and Ag devices were built using identical CQD films, we conclude that the loss of device performance is dominated by degradation at the Schottky contact. Ag is less reactive than Al[16] and results in a more stable Schottky contact with PbS nanocrystal film.

Unfortunately, use of an Ag cathode results in a low V_{oc} of 0.24 V compared with 0.42 V using the Al cathode. We sought a means to combine the high efficiency of the Al contact with an extended device lifetime. We believed that sandwiching a thin barrier layer between PbS nanocrystal film and the Al electrode might offer such a solution.

Introducing a thin LiF layer before Al electrode deposition had shown great value in organic photovoltaics (OPV)[17] and organic light emitting diodes (OLED),[18] enhancing both stability and performance. Various explanations of this phenomenon have been provided, including doping of the organic functional layer,[19] formation a dipole layer at the film/electrode interface,[17] and elimination of chemical reaction between Al and the organic film.[20] This concept seemed potentially worth adapting to the case of PbS CQDs films; though whether the benefits would translate was uncertain for a number of reasons. In OPV and OLEDs, the contact between the organic film and Al electrode is ohmic, while in the devices considered herein, it is a Schottky barrier acutely sensitive to traps. The PbS CQDs film is a mixture of inorganic PbS and organic ligands, in contrast with the purely organic case of OPV. Additionally, the CQD film top surface is innately rough on the multi-nanometer length scale of the nanoparticles themselves; and yet the most effective past reports of LiF barriers have employed sub-nanometer films.

We investigated a number of candidate interlayers including silicon monoxide (SiO), bismuth chloride ($BiCl_3$), and lithium fluoride (LiF). Introduction of SiO and $BiCl_3$ interlayers led to poorer device performance than pure Al contol device. The SiO interlayer increased series resistance and $BiCl_3$ interlayer reduced shunt resistance, suggesting both SiO and $BiCl_3$ have unfavorable interfacial properties. LiF, however, increased shunt resistance and reduced series resistance simultaneously. We found that a remarkably thin 0.8 nm LiF produced the best results whereas devices with thicker LiF (2–3 nm) suffered from low photocurrent.

The evolution of the performance of a ITO/PbS/LiF/Al/Ag device during ambient storage is summarized in Figure 1C. Introduction a 0.8 nm LiF thin layer significantly improved device stability in ambient compared with pure Al contact: after 7 days' storage in air, the EQE, V_{oc} and FF decreased by 13.9%, 16.2%, 22.8%, respectively, leading to an overall 45.4% reduction in MPCE. Assessed by the 80%-MPCE-lifetime metric, the device lifetime improved 6-fold, from 4 h to 24 h.

We further tested device durability under simultaneous and continuous 100 mW cm^{-2} AM1.5G illumination and current-voltage (I–V) scanning. As shown in Figure 2A, the unpackaged device exhibited an almost constant V_{oc} and a gradually decreased FF during the ~63-hour testing interval. The increased short-circuit photocurrent (J_{sc}) during the first ~37-hour testing period offset loss from FF decrease, leading to a maximum 6% gain in AM1.5G PCE in the first 10 hours. After 63-hour testing, the device lost 13% of its initial AM1.5G PCE. The stability of these unencapsulated devices in air and under solar illumination

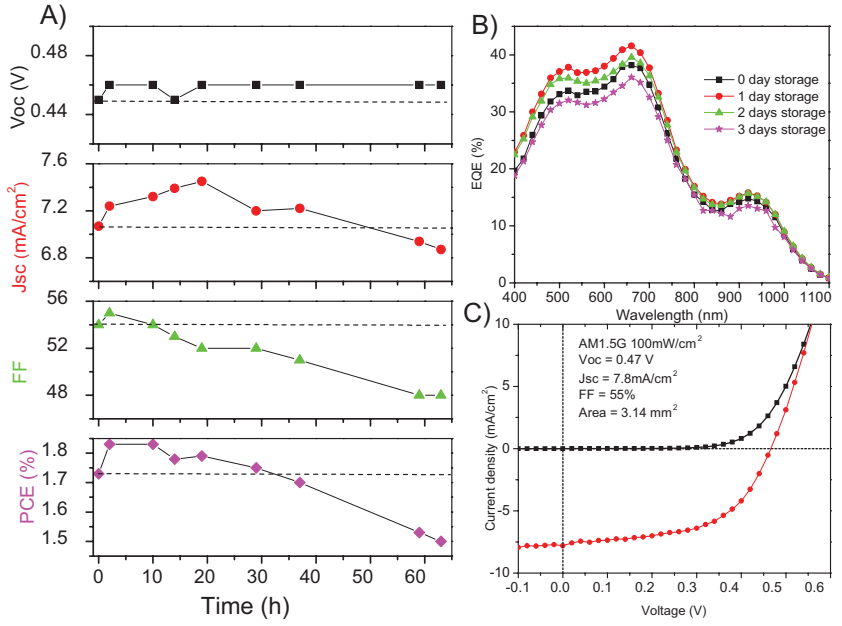

Figure 2. Stability and performance of unpackaged Glass/ITO/130 nm PbS/0.8 nm LiF/100 nm Al/100 nm Ag device. A) Device performance (V_{oc}, J_{sc}, FF, and AM1.5G PCE) measured in air under simultaneous and continuous I-V scanning (linear scan from −1 V to 1 V, 100 ms per 0.02 V) and simulated 100 mW cm^{-2} AM1.5G irradiation; B) Temporal evolution of EQE spectra of devices stored on in an air ambient; C) Representative device performance in the dark and under 100 mW cm^{-2} AM1.5G irradiation. Data shown in A and B are representative of 2 devices tested.

combined is comparable to the most stable unencapsulated OPV devices.[21,22]

The temporal evolution of the EQE spectra of our devices stored in ambient, as seen in Figure 2B, revealed an almost constant spectral shape and amplitude. The slightly increase in EQE during the first 2 days' storage agreed with the initial increase of J_{sc} observed above. There was no blue shift in the EQE spectrum near the excitonic peak, indicating that any incremental oxidation of our PbS nanocrystals was negligible.

The thin LiF layer increased the J_{sc}, V_{oc}, FF, and PCE of our PbS nanocrystal solar cells simultaneously, leading to a 2% AM1.5G PCE: V_{oc} of 0.47 V, J_{sc} of 7.8 mA cm^{-2} and FF of 55%, as shown in Figure 2C. Our device provides a combination of high efficiency and long lifetime not previously report among lead chalcogenide CQDs solar cells.[3,6–8,23]

We further explored the effect of LiF on device stability by tracking the shunt resistance (*Rp*), series resistance (*Rs*), rectification, and zero bias capacitance (C_0) of PbS CQDs device with and without 0.8 nm LiF layer during ambient storage. Al/Ag and LiF/Al/Ag electrode were evaporated onto the same PbS film to enable direct comparison. The results are summarized in Table 1. A high *Rp* (desirable) is associated with minimization of carrier recombination and of leakage current. A low *Rs* (desirable) is related to the decreased intrinsic resistance including resistances at the contacts. The C_0 indicates the exposed acceptor density in the region of the p-type semiconductor.[24,25]

As seen in Table 1, fresh devices incorporating 0.8 nm LiF showed larger *Rp* as well as smaller *Rs*. The LiF interlayer appears to reduce both recombination and resistance at the interface. More importantly, when both devices are stored in ambient for 4 days, the LiF-free contact experienced a 4-fold decrease in *Rp*, a 3-fold increase in *Rs*, a complete loss of rectification, and a 5-fold increase in C_0 indicating a large increase in acceptor density at the interface. We posit that reactions between PbS film and Al electrode generate traps near the interface that serve as recombination centers and also as acceptors. The LiF device saw a much more modest 2-fold loss in *Rp* and 2-fold increase in *Rs* and C_0. The rectification remains almost unaffected, confirming the Schottky contact was conserved after 4 days' ambient storage.

We now turn to depth-profile X-ray photoelectron spectroscopy (XPS) characterization elucidate further the reactivity of the interfaces. We used the same fabrication methods but built thinner devices (2 quantum dot layers), thinner metal contacts (5 nm Al, 8 nm Ag) and one device with 0.8 nm LiF but the other one without. Devices were left in an air ambient for two days and then the top contact was removed by sputtering[26] to reveal the semiconductor portion of the interface of interest for XPS characterization.

Depth-profile XPS characterization revealed that when no LiF was employed, the atomic concentration of O was consistently larger in both the Al layer and the PbS film compared to the case of the LiF device. We also analyzed the Al 2p core level features, ascribing the low binding energy peak at 72.7 eV to metallic Al and the high binding energy peak at 75.1 eV to hydrated Al_2O_3,[27] a reaction product of Al with oxygen in the presence of moisture. As shown in Figure 3, although Al suffered from severe oxidation in both film-characterization test structures, the metallic Al components in structures employing LiF were consistently larger than in the case of the LiF-free structure, suggesting that LiF did help to retard Al oxidation.

Table 1. Dependence of device parameters including parallel resistance (*Rp*), series resistance (*Rs*), rectification (defined as the dark current ratio at forward bias 1 V and revered bias −1 V) and zero bias capacitance (C_0) on the ambient storage time of PbS nanocrystal Schottky device with and without 0.8 nm LiF layer.

	Storage (H)	*Rp* (Ω)	*Rs* (Ω)	Rectification	C_0 (nF)
	0	2814	185	15	5.4
No	24	863	376	3	10.3
LiF	48	948	482	2	15.8
	72	917	634	1	23.9
	96	752	669	1	26.1
	0	4590	157	248	6.1
With	24	3372	210	270	9.1
LiF	48	2948	228	244	12.3
	72	2889	247	209	12.7
	96	2562	257	209	13.2

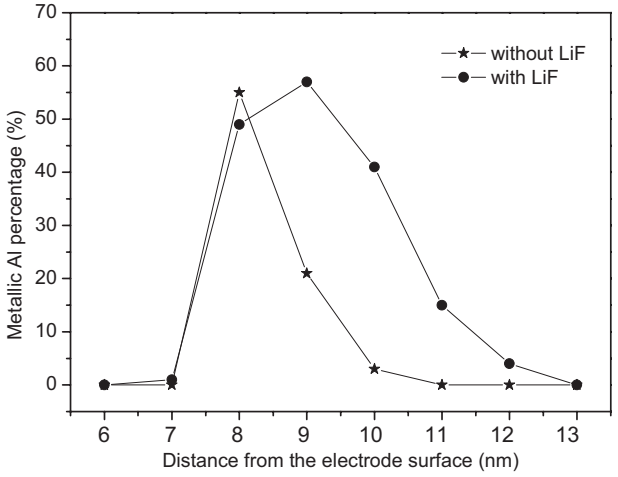

Figure 3. Metallic Al percentage calculated from Gaussian-Lorentzian fitting of depth-profile XPS experimental data on Multipak software: ITO/PbS/Al/Ag device without LiF (star) and ITO/PbS/LiF/Al/Ag device with LiF (circle). Sputtering started from Ag cap.

Two pathways exist by which oxygen and moisture can attack the Al layer and the PbS film: 1) vertical diffusion beginning at the top Ag layer; 2) lateral diffusion from the edges of the circular contacts in the plane. In PV devices having a 100 nm Ag cap, pathway 1 is unlikely and pathway 2 will dominate. However, the devices used in the XPS study employed a thin 8 nm Ag cap. We believe that the XPS study may therefore overestimate the oxidation rate compared to the PV device study.

The introduction of only 0.8 nm LiF thus produces marked benefits in retarding the diffusion of oxygen and the resultant progression of oxidation at the CQD film–metal interface. This remarkable result is nevertheless consistent with previous findings in OPV devices that 1 nm of LiF atop Al is sufficient to decrease Al oxidation significantly.[27] LiF provides good lattice match with Al over a broad range of orientations ($a_{LiF} = 4.02$ Å and $a_{Al} = 4.04$ Å) and thus a thin LiF coverage on Al dramatically retards the outward diffusion of Al in the oxidation process.[27]

In conclusion, we show that, in PbS colloidal quantum dot devices, degradation at the Al contact from interfacial reaction and oxidation is the main culprit in Schottky-CQDs solar cell degradation in air. Depth-profile XPS combined with optoelectronic device measurements indicate that, absent a LiF blocker, oxygen and moisture diffuse through the PbS film/Al interface and oxidize the Al electrode, causing device failure. Inserting a 0.8 nm LiF layer retards this degradation and extends unpackaged device lifetime over one order of magnitude to tens of hours in air under solar illumination and results in the first PbS CQDs device having AM1.5G PCE of 2%.

Experimental

PbS CQDs ($\lambda_{exciton} \sim 930$ nm) were synthesized as follows: 0.45 g PbO, 1.5 mL oleic acid, and 16.5 mL ODE were mixed and heated it to 120 °C to produce a clear solution. To this solution 210 μL bis(trimethylsilyl) sulfide in 10 mL ODE were swiftly injected. The solution was slowly cooled and then washed repeatedly by suspension in toluene and precipitation using acetone. After isolation, 1 mL oleylamine was added and the mixture was incubated for 2 days in a glove box. After another thrice methanol wash, PbS CQDs were redispersed in octane to produce a 10 mg mL^{-1} solution.

PbS CQD films were fabricated in an air ambient using a layer-by-layer deposition technique. Each iteration in the layer-by-layer deposition consisted of five steps: i) 5 drops of 10 mg mL^{-1} PbS octane solution; ii) 5 drops of 1% EDT solution; iii) 10 drops of anhydrous acetonitrile; iv) 10 drops of anhydrous octane; v) 10 s air drying. The resulting films were (130 ± 10) nm thick measured using a Dektak profilometer. Films were stored in a desiccator filled with N_2 for 1–4 h and then annealed at 90 °C in air for 5 min before electrode deposition.

Electrodes were deposited using thermal evaporation in an Edwards 306 evaporator with a pressure of 10^{-5} Torr. 0.8 nm LiF was deposited at a rate of 0.04–0.08 nm s^{-1}, followed by 100 nm Al and 100 nm Ag evaporation, both at a rate of 0.5 nm s^{-1}. A shadow mask was used to define a 4 × 4 array of 1.84 mm diameter circular contacts.

We calibrated the thickness of LiF as follows. We mounted 4 pieces of clean bare glass at different positions on top of the LiF source and then deposited LiF onto the glass. Four such calibration runs were carried out. In each run, a different thickness of LiF was evaporated onto the glass. We used a surface profilometer to measure the film thickness. In this way we determined the scaling factor between the nominal thickness and the actual and used it to calculate the real LiF thickness.

I–V measurements were performed using a Keithley 2400 sourcemeter. The Oriel solar simulator calibrated by Melles-Griot broad-band power meter was used to simulate the AM1.5G solar spectrum at 1 sun intensity. In EQE spectral measurements, spectral intensity was obtained using a Newport optical power meter and current was measured using a Stanford Research SR830 lock-in amplifier. XPS measurement employed the ESCA 5500 system using Mg Kα source. The in situ peel-off technique was applied by sputtering the sample using a 3 keV Ar^+-ion beam at a 60° incidence angle to expose the buried interface.

Acknowledgements

R. Debnath acknowledges the e8 scholarship. This publication was supported in part by Award No. KUS-I1-009-21 made by King Abdullah University of Science and Technology (KAUST).

Received: September 21, 2009
Revised: October 13, 2009
Published online: January 7, 2010

[1] I. Gur, N. A. Fromer, M. L. Geier, A. P. Alivisatos, *Science* **2005**, *310*, 462.
[2] Y. Wu, C. Wadia, W. Ma, B. Sadtler, A. P. Alivisatos, *Nano Lett.* **2008**, *8*, 2551.
[3] K. W. Johnston, A. G. Pattantyus-Abraham, J. P. Clifford, S. H. Myrskog, D. D. MacNeil, L. Levina, E. H. Sargent, *Appl. Phys. Lett.* **2008**, *92*, 151115.
[4] E. J. D. Klem, D. D. MacNeil, P. W. Cyr, L. Levina, E. H. Sargent, *Appl. Phys. Lett.* **2007**, *90*, 183113.
[5] D. A. R. Barkhouse, A. G. Pattantyus-Abraham, L. Levina, E. H. Sargent, *ACS Nano* **2008**, *2*, 2356.
[6] J. M. Luther, M. Law, M. C. Beard, Q. Song, M. O. Reese, R. J. Ellingson, A. J. Nozik, *Nano Lett.* **2008**, *8*, 3488.
[7] G. Koleilat, L. Levina, H. Shukla, S. H. Myrskog, S. Hinds, A. G. Pattantyus-Abraham, E. H. Sargent, *ACS Nano* **2008**, *2*, 833.
[8] W. Ma, J. M. Luther, H. Zheng, Y. Wu, A. P. Alivisatos, *Nano Lett.* **2009**, *9*, 1699.
[9] K. W. Johnston, A. G. Pattantyus-Abraham, J. P. Clifford, S. H. Myrskog, S. Hoogland, H. Shukla, E. J. D. Klem, E. H. Sargent, *Appl. Phys. Lett.* **2008**, *92*, 122111.

[10] B. Q. Sun, A. T. Findikoglu, M. Sykora, D. J. Werder, V. I. Klimov, *Nano Lett.* **2009**, *9*, 1235.
[11] G. Konstantatos, I. Howard, A. Fischer, S. Hoogland, J. Clifford, E. Klem, L. Levina, E. H. Sargent, *Nature* **2006**, *442*, 180.
[12] G. Konstantatos, J. Clifford, L. Levina, E. H. Sargent, *Nat. Photonics* **2007**, *1*, 531.
[13] G. Konstantatos, L. Levina, A. Fischer, E. H. Sargent, *Nano Lett.* **2008**, *8*, 1446.
[14] J. M. Luther, M. Law, Q. Song, C. L. Perkins, M. C. Beard, A. J. Nozik, *ACS Nano* **2008**, *2*, 271.
[15] E. Lifshitz, M. Brumer, A. Kigel, A. Sashchiuk, M. Bashouti, M. Sirota, E. Galun, Z. Burshtein, A. Q. Le Quang, I. Ledoux-Rak, J. Zyss, *J. Phys. Chem. B* **2006**, *110*, 25356.
[16] J. G. R. Briggs, *Science in Focus, Chemistry for GCE'O' Level*, Pearson Education, New Jersey, USA **2005**, p. 172.
[17] C. J. Brabec, S. E. Shaheen, C. Winder, N. S. Sariciftci, P. Denk, *Appl. Phys. Lett.* **2001**, *80*, 1288.
[18] L. S. Hung, C. W. Tang, M. G. Mason, *Appl. Phys. Lett.* **1997**, *70*, 152.
[19] K. R. Choudhury, J. Yoon, F. So, *Adv. Mater.* **2008**, *20*, 1456.
[20] M. G. Mason, C. W. Tang, L. S. Hung, P. Raychaudhuri, J. Madathil, L. Yan, Q. T. Le, Y. Gao, S. T. Lee, L. S. Liao, L. F. Cheng, W. R. Salaneck, D. A. Santos, J.-L. Brédas, *J. Appl. Phys.* **2001**, *89*, 2756.
[21] K. Lee, J. Y. Kim, S. H. Park, S. H. Kim, S. Cho, A. J. Heeger, *Adv. Mater.* **2007**, *19*, 2445.
[22] T. Kuwabara, T. Nakayama, K. Uozumi, T. Yamaguchi, K. Takahashi, *Sol. Energy Mater. Sol. Cells* **2008**, *92*, 1476.
[23] E. H. Sargent, *Nat. Photonics* **2009**, *3*, 325.
[24] J. P. Clifford, K. W. Johnston, L. Levina, E. H. Sargent, *Appl. Phys. Lett.* **2007**, *91*, 253117.
[25] V. Shrotriya, Y. Yang, *J. Appl. Phys.* **2005**, *97*, 054504.
[26] D. Grozea, A. Turak, X. D. Feng, Z. H. Lu, D. Johnson, R. Wood, *Appl. Phys. Lett.* **2002**, *81*, 3173.
[27] A. Turak, C. J. Huang, D. Grozea, Z. H. Lu, *J. Electrochem. Soc.* **2007**, *154*, H691.